Critical adsorption profiles around a sphere and a cylinder in a fluid at criticality: Local functional theory

Shunsuke Yabunaka[1] and Akira Onuki[2]
[1]*Fukui Institute for Fundamental Chemistry, Kyoto University, Kyoto 606-8103, Japan*
[2]*Department of Physics, Kyoto University, Kyoto 606-8502, Japan*
(Received 23 June 2017; published 18 September 2017)

We study universal critical adsorption on a solid sphere and a solid cylinder in a fluid at bulk criticality, where preferential adsorption occurs. We use a local functional theory proposed by Fisher *et al.* [M. E. Fisher and P. G. de Gennes, C. R. Acad. Sci. Paris Ser. B **287**, 207 (1978); M. E. Fisher and H. Au-Yang, Physica A **101**, 255 (1980)]. We calculate the mean order parameter profile $\psi(r)$, where r is the distance from the sphere center and the cylinder axis, respectively. The resultant differential equation for $\psi(r)$ is solved exactly around a sphere and numerically around a cylinder. A strong adsorption regime is realized except for very small surface field h_1, where the surface order parameter $\psi(a)$ is determined by h_1 and is independent of the radius a. If r considerably exceeds a, $\psi(r)$ decays as $r^{-(1+\eta)}$ for a sphere and $r^{-(1+\eta)/2}$ for a cylinder in three dimensions, where η is the critical exponent in the order parameter correlation at bulk criticality.

DOI: 10.1103/PhysRevE.96.032127

I. INTRODUCTION

Surface critical phenomena and phase transitions have long been studied in various near-critical systems [1–3]. In particular, the critical adsorption occurs when a near-critical system in a single-phase state is in contact with a distinctly different boundary [4–7]. In experiments, it has been studied intensively in near-critical binary fluid mixtures on a solid surface or a noncritical vapor-liquid interface at constant pressure [8–15]. Much attention has also been paid to preferential adsorption on colloidal particles [16–18], which is known to give rise to colloid aggregation [16,19,20]. We mention a few experiments on critical adsorption of supercritical pure fluids [21–23]. There have been a large number of theoretical papers on the surface effects in the semi-infinite case [1–3,12,24–30] and on curved surfaces [6,31–34].

The order parameter in nearly incompressible binary mixtures is the deviation $\psi = c - c_c$ of the concentration c from its critical value c_c. Because a solid surface interacts with the two components differently, there can be preferential adsorption on the surface. In such situations, the mean order parameter $\psi(z)$ on a planar surface (averaged over the thermal fluctuations) has been measured [9–15], where z is the distance from the surface. From the Fisher–de Gennes scaling theory [4], an algebraic slow decay follows [7,12,25,28],

$$\psi(z) = Az^{-(1+\eta)/2}, \tag{1}$$

in three dimensions. Here, A is a constant and η is the critical exponent ($\ll 1$) for the correlation function of the critical fluctuations at bulk criticality. If the bulk correlation length ξ_B is finite slightly away from the bulk criticality, the above form holds for $z < \xi_B$ and $\psi(z)$ decays exponentially as $\exp(-z/\xi_B)$ for larger z.

On the other hand, to examine the critical adsorption on a sphere, de Gennes [6] used a local functional theory by himself, Fisher, and Au-Yang [4,5] at bulk criticality. He calculated the profile $\psi(r)$, where r is the distance from the center of a sphere with radius a. Setting $\eta = 0$, he found that $\psi(r)$ largely drops in the range $a < r < 2a$ and slowly decays as r^{-1} for $r > 2a$ in strong adsorption. With increasing a, this strong adsorption condition can easily be realized even for small surface field h_1. However, in their coarse-grained free energy, surface dependence of the critical fluctuations is neglected in accounting for the renormalization effect. As a result, it does not describe the surface critical behaviors appearing at very small h_1 [2,15,24–28]. Nevertheless, their free energy provides a simple reasonable description of the critical adsorption in the strong adsorption regime.

In this paper, we examine the adsorption on a sphere and a cylinder at bulk criticality with the local functional theory [4,5]. For a sphere, we find an exact solution of the equation for $\psi(r)$ used by de Gennes [6]. We confirm his results and derive additional relations. For a cylinder, we examine it numerically and find asymptotic behaviors of its solutions. On the other hand, in colloidal systems with a near-critical solvent, the thick-adsorption regime $a < \xi_B$ can be realized for relatively small a in close vicinity of the critical point. However, in this regime, we are aware of only one experimental report by Omari *et al.* [17], so its physical picture remains largely unexplored. Hence, this paper can be a starting point in the research in this direction.

The organization of this paper is as follows. In Sec. II, we will present the local functional theory of a critical fluid in the presence of a solid surface. In Sec. III, we examine the order parameter profiles near a planar wall, a sphere, and a cylinder. In Sec. IV, we will comment on the effect of motions of colloidal particles on the surrounding critical adsorption for $a < \xi_B$.

II. LOCAL FUNCTIONAL THEORY

We suppose a solid surface in a binary fluid mixture without ions, which is at its critical point in the bulk at a given pressure. The radius a of the sphere or the cylinder is much longer than the molecular length a_0($\sim$3 Å typically). The mean order parameter near a solid wall is denoted by ψ, which tends to 0 far from the wall.

At bulk criticality, Fisher, de Gennes, and Au-Yang [4,5] proposed a local functional theory, where the singular free

energy consists of two terms as

$$f = B_0|\psi|^{1+\delta} + \tfrac{1}{2}C_0|\psi|^{-\eta\nu/\beta}|\nabla\psi|^2. \quad (2)$$

Here, B_0 and C_0 are positive constants. The spatial variations of ψ near the walls are simply treated by the second gradient term. We use the usual, bulk critical exponents δ, η, ν, and β for Ising-like systems. In three dimensions, we have $\beta \cong 0.33$, $\nu \cong 0.630$, and $\eta \cong 0.03$-0.04. For general space dimensionality d ($2 \leqslant d \leqslant 4$), they satisfy the exponent relations [35],

$$\delta = (d+2-\eta)/(d-2+\eta), \quad 2\beta/\nu = d-2+\eta. \quad (3)$$

The ratio of the second term to the first term in f can be expressed as $\xi(\psi)^2|\nabla\psi|^2/4\psi^2$ [4,5], where

$$\xi(\psi) = b_0|\psi|^{-\nu/\beta} \quad (4)$$

is the ψ-dependent correlation length at $T = T_c$ with

$$b_0 = (2C_0/B_0)^{1/2}. \quad (5)$$

Here, b_0 is a microscopic length if ψ is the concentration deviation. This $\xi(\psi)$ should be longer than the molecular length a_0. The free energy in Eq. (2) is a renormalized one, where the thermal fluctuations shorter than $\xi(\psi)$ have been coarse-grained, leading to the fractional powers $|\psi|^{1+\delta-4}$ and $|\psi|^{-\eta\nu/\beta}$ in f. As a result, it cannot be used to describe variations on scales shorter than $\xi(\psi)$.

From the two-scale factor universality [35–37], the following combination is a universal number:

$$A_c = \xi(\psi)^d B_0|\psi|^{1+\delta}/k_{\rm B}T_c = b_0^3 B_0/k_{\rm B}T_c, \quad (6)$$

where we use $1+\delta = d\nu/\beta$. Then, $B_0 = A_c k_{\rm B}T_c/b_0^3$ and $C_0 = A_c k_{\rm B}T_c/2b_0$. If we use the ϵ expansion method of the renormalization group theory, we obtain $A_c = 18/(\pi^2\epsilon) + \cdots$ to first order in $\epsilon = 4-d$ [30,38].

In the presence of a solid surface, the free energy functional consists of bulk and surface parts as [1]

$$F = \int d\boldsymbol{r}\, f + \int dS f_s, \quad (7)$$

where the integral in the first term is performed in the fluid and the second term is the surface integral of the surface free energy $f_s(\psi)$, with dS being the surface element. In this paper, we assume the linear form,

$$f_s = -h_1\psi, \quad (8)$$

where h_1 is the surface field equal to the surface free energy difference between the two components per unit area. We set $h_1 > 0$ and have $\psi > 0$. (For $h_1 < 0$, we perform the sign changes: $\psi \to -\psi$ and $h_1 \to -h_1$.) Assuming a significant size of h_1, we neglect the second order term of the form $c\psi^2$ in f_s [1,2].

Following de Gennes [6], we may replace $1+\delta$ by 6 and $|\psi|^{-\eta\nu/\beta}$ by 1 in f setting $d = 3$ and $\eta = 0$. Then, minimization of F yields the equilibrium conditions,

$$\nabla^2\psi = (6B_0/C_0)\psi^5 \quad \text{(in fluid)}, \quad (9)$$

$$\boldsymbol{n}\cdot\nabla\psi = -h_1/C_0 \quad \text{(on surface)}, \quad (10)$$

where $\boldsymbol{n}$ is the outward normal unit vector on the surface. We also require $\psi \to 0$ far from the solid surface where the fluid is at criticality.

To be precise, we do not need the above approximation ($1+\delta \to 6$ and $|\psi|^{-\eta\nu/\beta} \to 1$) to obtain Eqs. (9) and (10). In fact, for general d and nonvanishing η, we introduce the following variable φ by

$$\varphi = |\psi|^{-\eta/2\beta}\psi \quad \text{or} \quad \psi = |\varphi|^{\eta_1}\varphi, \quad (11)$$

where $\eta_1 = \eta/(d-2)$. We then find $f = B_0|\varphi|^{2d/(d-2)} + C_0(1+\eta_1)^2|\nabla\varphi|^2/2$. See Appendix A for more details.

Borjan and Upton [28] calculated $\psi(z)$ on a planar wall using a local functional theory in good agreement with results of Monte Carlo simulations. Okamoto and one of the present authors (A.O.) [30] constructed a local functional theory in strong adsorption, which can be used for nonvanishing $T - T_c$ and ψ (including the interior region of the coexistence curve). We could then study phase separation between two parallel plates [39] and bridging transitions between two colloidal particles [34,40].

In semidilute polymer solutions at the theta condition, an order parameter $\psi = \sqrt{\phi}$ obeys the same equation as Eq. (9) [41], where ϕ is the monomer volume fraction. This is because the free energy contains a gradient term proportional to $|\nabla\phi|^2/\phi$ and no ϕ^2 term at the theta condition. Thus, our results can also be used to describe polymer adsorption and depletion on solid walls (including colloid surfaces).

III. PROFILES NEAR A PLANAR WALL, A SPHERE, AND A CYLINDER

A. Planar surface

We first consider $\psi(z)$ in the semi-infinite region $z > 0$ on a planar surface at $z = 0$, where the z axis is perpendicular to the surface. Solving Eq. (9), we find

$$\psi(z) = [b_0/4(z+z_0)]^{1/2}, \quad (12)$$

where z_0 is a length determined by h_1 from Eq. (10) as

$$z_0 = b_0^{1/3}(C_0/4h_1)^{2/3}. \quad (13)$$

For general d and η, the exponent $1/2$ in Eq. (12) is changed to $\beta/\nu = (d-2+\eta)/2$ (see Appendix A). Thus, Eq. (1) follows for $z \gg z_0$ at $d = 3$.

The above z_0 exceeds the microscopic length a_0 for

$$b_0 h_1/C_0 \sim b_0^2 h_1/k_{\rm B}T_c < 1, \quad (14)$$

where we assume $a_0 \sim b_0$. Then, in the range $a_0 < z < z_0$, ψ assumes the following surface value:

$$\psi_s = (b_0/z_0)^{1/2}/2 = (b_0 h_1/2C_0)^{1/3}, \quad (15)$$

which is smaller than 1 under Eq. (14). If the reverse inequality $b_0^2 h_1/k_{\rm B}T_c > 1$ holds, the algebraic behavior (12) holds down to a_0 and the surface concentration saturates to 1. For $z_0 \ll \xi_{\rm B}$, the z integral of $\psi(z)$ yields the excess adsorption $\Gamma_{1d} \sim \xi_{\rm B}^{1-\beta/\nu}$ (independent of h_1).

If we define the correlation length near the surface by $\xi_s = \xi(\psi_s) = b_0\psi_s^{-2}$ from Eq. (4), we have $z_0 = \xi_s/2 > b_0 \sim a_0$ under Eq. (14). If we recover η, we have the scaling relations $\xi_s \propto h_1^{-\nu/(2\nu-\beta)}$ and $\psi_s \propto \xi_s^{-\beta/\nu} \propto h_1^{\beta/(2\nu-\beta)}$. That is,

with Eqs. (2) and (8) at significant h_1, there appear no special surface critical exponents such as Δ_1 and β_1 [25,28]. However, for very small h_1, it is known that the effect of the surface on the critical fluctuations becomes relevant [24,26,27]. See the comment in Sec. I and experiments in critical mixtures at very small h_1 [13,15].

B. Sphere

We fix the position of an isolated solid sphere with radius a in a near-critical fluid, where ψ depends only on the distance r from the sphere center. Experimentally, the bulk correlation length ξ_B can much exceed a, where our theory can be used in the space region $a < r < \xi_B$.

Starting with Eqs. (9) and (10), we introduce a scaled order parameter Ψ and a scaled surface field H_1 by

$$\Psi = 12^{1/4} b_0^{-1/2} a^{1/2} \psi, \tag{16}$$

$$H_1 = 12^{1/4} b_0^{-1/2} a^{3/2} h_1 / C_0, \tag{17}$$

where $H_1 = 3^{1/4}(a/2z_0)^{3/2}$ in terms z_0 in Eq. (13) [6]. Using the scaled distance $x = r/a$, we obtain

$$\Psi'' + 2x^{-1}\Psi' = \Psi^5, \tag{18}$$

$$\Psi' = -H_1 \quad (x = 1), \tag{19}$$

with $\Psi(\infty) = 0$. Here, $\Psi' = d\Psi/dx$ and $\Psi'' = d^2\Psi/dx^2$.

Remarkably, Eq. (18) can be solved exactly as

$$\Psi(x) = 3^{1/4} x_0^{1/2} / \left(x^2 - x_0^2\right)^{1/2}, \tag{20}$$

which diverges as $x \to x_0$, with x_0 being a lower bound in the range [0,1] (inside the sphere). In terms of x_0, H_1 and $\Psi_1 = \Psi(1)$ are expressed as

$$H_1 = \Psi_1 / \left(1 - x_0^2\right) = 3^{1/4} x_0^{1/2} / \left(1 - x_0^2\right)^{3/2}. \tag{21}$$

We plot $\Psi(x)$ and $x\Psi(x)$ in Fig. 1, while we show the relations among x_0, H_1, Ψ_1, and α in Fig. 2 [see Eq. (26) for α]. In Appendix A, we shall see the exact profile around a sphere at bulk criticality for general d and η using Eq. (3). See remark (i) in Sec. V also.

We are interested in the strong adsorption regime $H_1 \gg 1$, which is realized for $b_0 h_1 / C_0 \gg (b_0/a)^{3/2}$ from Eq. (17). For large a, this condition can be realized even under Eq. (14). From Eq. (21), we express x_0 and Ψ_1 in terms of H_1 in the weak and strong adsorption limits as

$$x_0 \cong 3^{-1/2} H_1^2, \quad \Psi_1 \cong H_1 \quad (H_1 \ll 1), \tag{22}$$

$$1 - x_0^2 \cong 3^{1/6} H_1^{-2/3}, \quad \Psi_1 \cong 3^{1/6} H_1^{1/3} \quad (H_1 \gg 1). \tag{23}$$

For $H_1 \gg 1$, x_0 approaches 1 and Ψ_1 grows. From Eqs. (16) and (21)–(23), the surface order parameter ψ_s in the original units behaves as follows:

$$\psi_s = \psi(a) \cong a h_1 / C_0 \quad (H_1 \ll 1), \tag{24}$$

$$\cong (b_0 h_1 / 2C_0)^{1/3} \quad (H_1 \gg 1). \tag{25}$$

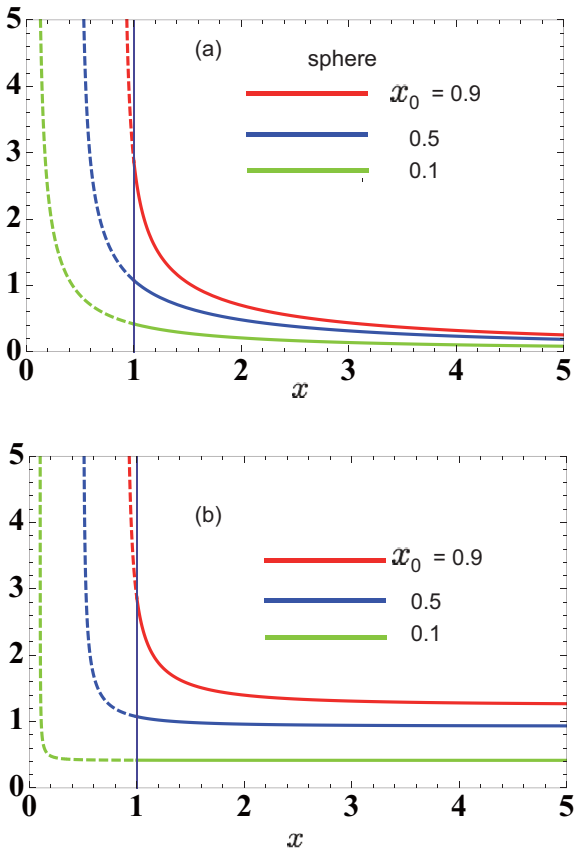

FIG. 1. (a) $\Psi(x)$ and (b) $x\Psi(x)$ as functions of $x = r/a$ around a solid sphere with radius a in a fluid at criticality. They are written according to the exact solution (20) including the sphere interior ($x < 1$). Three curves are obtained for (from top to bottom) $x_0 = 0.9$, 0.5, and 0.1, for which $(H_1, \Psi_1, \alpha) = (15.1, 2.86, 1.64)$, $(1.43, 1.08, 1.22)$, and $(0.423, 0.418, 0.548)$, respectively. Here, $\Psi(x)$ diverges as $x \to x_0$ and decays as α/x with $\alpha = 3^{1/4} x_0^{1/2}$ for $x > 2$.

We can derive Eq. (24) from $\psi \cong \psi_s a/r$ $(r > a)$ for $H_1 \ll 1$. Notice that Eq. (25) is of the same form as Eq. (15) for a planar wall. See Appendix A for this point.

For $x \gg x_0$, we find the slow decay $\Psi \cong \alpha/x$ with [6]

$$\alpha = 3^{1/4} x_0^{1/2}. \tag{26}$$

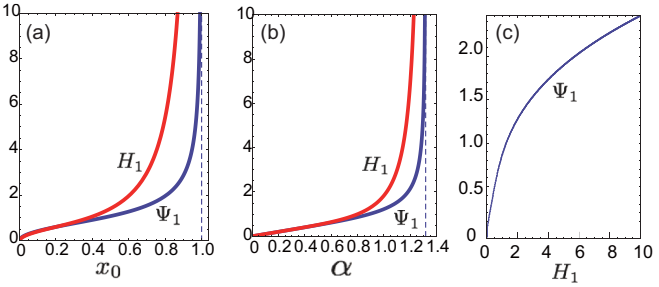

FIG. 2. (a) H_1 and Ψ_1 vs x_0 from Eq. (21), where $0 < x_0 < 1$. (b) H_1 and Ψ_1 vs $\alpha = 3^{1/4} x_0^{1/2} (< 3^{1/4})$. (c) Ψ_1 vs H_1, which behaves as in Eqs. (22) and (23).

This α should not be confused with the critical exponent α. In the original units, this decay is rewritten as

$$\psi(r) \cong (x_0 b_0/2)^{1/2} a^{1/2} r^{-1}. \tag{27}$$

For $H_1 \ll 1$, the above behavior holds in the whole fluid, so $\psi(r) \cong \psi_s a/r$ for $r > a$ (see Fig. 1). For $H_1 \gg 1$, it holds for r/a considerably larger than 1, say, for $x = r/a \gtrsim 2$, where the correlation length in Eq. (4) is estimated as

$$\xi(\psi) \sim r^2/a \quad (r \gtrsim 2a). \tag{28}$$

If ξ_B is finite, the above relation is meaningful for $r < (a\xi_B)^{1/2}$. In this case, from Eqs. (20) and (23), we calculate the drop of $\psi(r)$ in the region $1 < r/a < 2$ as

$$\psi(2a)/\psi(a) = \Psi(2)/\Psi(1) \sim \left(1 - x_0^2\right)^{1/2} \sim H_1^{-1/3}, \tag{29}$$

which is smaller than 1 for $H_1 \gg 1$. If η is recovered, Eq. (11) leads to $\psi \sim (b_0/a)^{(1+\eta)/2}\Psi^{1+\eta}$ so that

$$\psi(r) \sim (x_0 b_0 a)^{(1+\eta)/2} r^{-(1+\eta)}. \tag{30}$$

See Eq. (A4) in Appendix A. We may also consider the total excess adsorption, written as Γ_{tot}, which is the space integral of ψ outside the sphere. For $H_1 \gg 1$ and $a \ll \xi_B$, the contribution from the region $r > 2a$ is dominant and is estimated from Eq. (30) as [33]

$$\Gamma_{tot} \sim a^{(1+\eta)/2} \xi_B^{2-\eta}. \tag{31}$$

It is worth noting that the pair correlation function of the critical fluctuations of ψ decays at criticality as [35]

$$g_{th}(r) = C_{th} r^{-(d-2+\eta)}. \tag{32}$$

Setting $d = 3$ and $\eta = 0$, we find $C_{th} \cong k_B T_c/C_0 = 2b_0/A_c$ in terms of C_0 in Eq. (2). Interestingly, $\psi(r)$ in Eq. (30) depends on r in the same manner as $g_{th}(r)$. However, the coefficient in $\psi(r)$ grows as $a^{(1+\eta)/2}$ with increasing a in the strong adsorption regime.

Originally, de Gennes [6] numerically calculated a special solution of Eq. (18), written as $\Phi_{PG}(x)$, which behaves as x^{-1} for $x \gg 1$. He constructed the other solutions by scaling $\Phi_\alpha(x) = \Phi_{PG}(x/\alpha^2)/\alpha$ [see Eq. (36)], which tends to α/x for large x. In our theory, Eq. (20) gives $\Phi_{PG}(x) = (x^2 - 1/3)^{-1/2}$ with $x_0 = 3^{-1/2} \cong 0.58$. Burkhardtt and Eisenriegler [31] found the profile in Eq. (20) particularly for $x_0 = 1$ (where $H_1 = \infty$) using conformal mapping of the results for the half space.

C. Cylinder

We next consider a cylindrical wire fixed in a critical fluid. It is infinitely elongated and ψ depends only on the distance r from the cylindrical axis. We use the normalized Ψ and H_1 in Eqs. (16) and (17). In terms of $x = r/a$, Eq. (9) becomes

$$\Psi'' + x^{-1}\Psi' = \Psi^5. \tag{33}$$

The boundary condition at $x = 1$ is given by Eq. (19) and we assume $\Psi(\infty) = 0$. In particular, for $H_1 = 2^{-3/2} \cong 0.354$, we find a special solution given by

$$\Psi_{sp}(x) = (2x)^{-1/2}. \tag{34}$$

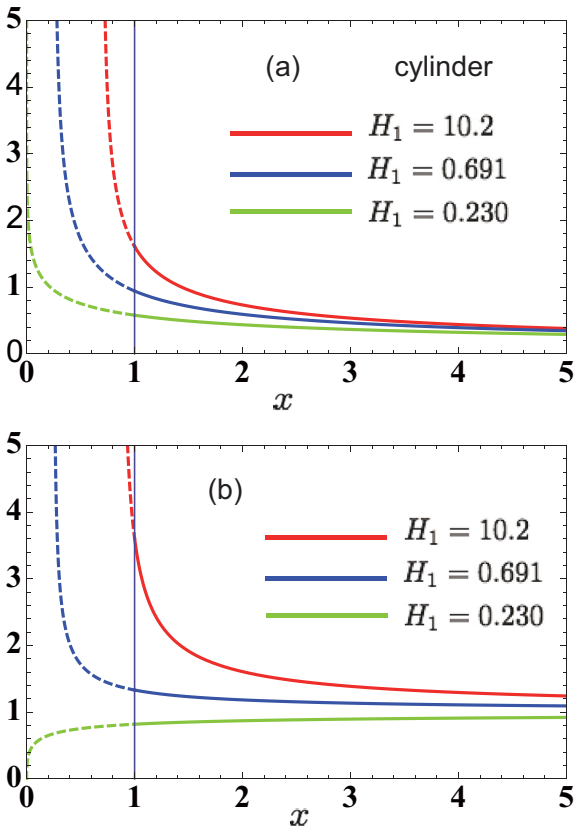

FIG. 3. (a) $\Psi(x)$ and (b) $\sqrt{2x}\Psi(x)$ as functions of $x = r/a$ around a solid cylinder with radius a in a fluid at criticality. They are numerically obtained from Eqs. (33) and (19) for $H_1 = 10.2$, 0.691, and 0.230, for which $\Psi_1 = 1.61$, 0.941, and 0.579, respectively. They are written in the cylinder exterior and interior. For $H_1 > 2^{-3/2} = 0.354$, $\Psi(x)$ diverges as $x \to x_0$ as in Eq. (40), where x_0 is 0.871 for $H_1 = 10.2$ and 0.248 for $H_1 = 0.691$. For $H_1 < 2^{-3/2}$, $\Psi(x)$ diverges as $x \to 0$ as in Eq. (41). In (b), $\sqrt{2x}\Psi(x)$ tends to 1 at large x as in Eq. (38) for any H_1.

In the original units, Eq. (16) gives

$$\psi_{sp} = 12^{-1/4}(b_0/a)^{1/2}\Psi_{sp} = 3^{-1/4}(b_0/4r)^{1/2}, \tag{35}$$

which is independent of a. If r here is replaced by $z + z_0$, this solution is smaller than the one-dimensional profile (12) by $3^{-1/4}$. For general d and η, we obtain $\psi_{sp} \propto r^{-(d-2+\eta)/2}$ (see Appendix A). However, we can solve Eq. (33) only numerically for general H_1. In Fig. 3, we plot $\Psi(x)$ and $(2x)^{1/2}\Psi(x)$ for three values of H_1, where the latter behaves differently for positive and negative $H_1 - 2^{-3/2}$. In Fig. 4, we display Ψ_1 vs H_1 for these two cases separately.

Let $\Psi_0(x)$ be a (numerically calculated) special solution of Eq. (33) with $H_1 \neq 2^{-3/2}$. Then, other solutions of Eq. (33) can be obtained by de Gennes' scaling [6],

$$\Psi_\lambda(x) = \lambda^{1/2}\Psi_0(\lambda x), \tag{36}$$

where α in Ref. [6] is replaced by $\lambda^{-1/2}$. For $\lambda < 1$, we need to know the behavior of $\Psi_0(x)$ in the range $x < 1$. We can then relate $\Psi_1 = \Psi_\lambda(1)$ and H_1 by eliminating λ in the following relations:

$$\Psi_1 = \lambda^{1/2}\Psi_0(\lambda), \quad H_1 = -\lambda^{3/2}\Psi_0'(\lambda). \tag{37}$$

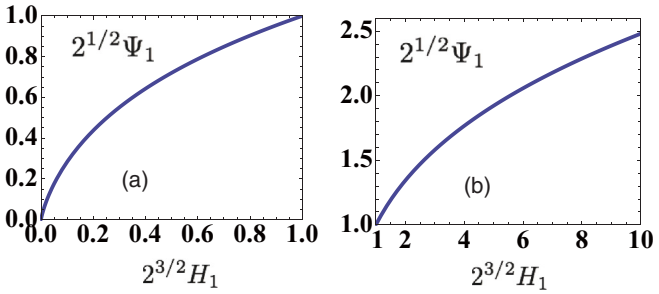

FIG. 4. $2^{1/2}\Phi_1$ vs $2^{3/2}H_1$ for a cylinder for (a) $H_1 < 2^{-3/2}$ and (b) $H_1 > 2^{-3/2}$. These curves are calculated from Eq. (37) using two special solutions in these cases. The curves behave as in Eqs. (42) and (43).

From analysis in Appendix B, we further find the following:

(i) For any H_1, Ψ behaves for $x \gg 1$ as

$$\Psi(x) = (2x)^{-1/2}[1 + G_1 x^{-\zeta} + \cdots], \tag{38}$$

where G_1 is a constant and $\zeta = (\sqrt{5}-1)/2$. Thus, $\Psi(x) \to \Psi_{\rm sp}(x)$ slowly for any H_1, which is consistent with the slow decay of $(2x)^{1/2}\Psi(x)$ in Fig. 3(b). In particular, for small $H_1 - 2^{-3/2}$, we obtain the linear relations

$$G_1 \cong 5^{-1/2}(2^{3/2}H_1 - 1) \cong 2^{1/2}\Psi_1 - 1. \tag{39}$$

The excess adsorption per unit length is of the order of $\xi_{\rm B}^{(3-\eta)/2}$ and is independent of a for $a \ll \xi_{\rm B}$.

(ii) If $H_1 > 2^{-3/2}$, $\Psi(x)$ is larger than $(2x)^{-1/2}$ for any $x > x_0$ with $0 < x_0 < 1$. It diverges as $x \to x_0$ as

$$\Psi(x) \cong 3^{1/4}[2x\ln(x/x_0)]^{-1/2}. \tag{40}$$

For example, we have $x_0 = 0.248$ for $H_1 = 0.691$. Use of Eq. (36) yields other solutions diverging at $\lambda^{-1}x_0$ [42].

(iii) If $H_1 < 2^{-3/2}$, we have $\Psi(x) < (2x)^{-1/2}$ for any $x > 0$. As $x \to 0$, we find

$$\Psi(x) \cong 2^{-1/2}(A_1 - A_2 \ln x), \tag{41}$$

where A_1 and A_2 are constants. For example, $A_1 = -1.27$ and $A_2 = 1.34$ for $H_1 = 0.3$ [42].

Now, in Eq. (37), we set $\Psi_0(\lambda) = 3^{1/4}[2\lambda\ln(\lambda/x_0)]^{-1/2}$ from Eq. (40) and $\Psi_0(\lambda) = 2^{-1/2}(A_1 - A_2\ln\lambda)$ from Eq. (41). Here, the former (latter) yields the limiting behavior for large (small) H_1 as follows:

$$\Psi_1 \cong H_1(A_3 - 2\ln H_1) \quad (H_1 \ll 1), \tag{42}$$

$$\cong 3^{1/6}H_1^{1/3} \quad (H_1 \gg 1), \tag{43}$$

where $A_3 = A_1/A_2 + \ln(A_2^2/2) \cong -1.05$ [42]. Notice that Eq. (43) coincides with the second relation in Eq. (23), so the surface order parameter ψ_s is again given by Eq. (15) or Eq. (25) in the strong adsorption regime. In fact, from Eq. (40), we find $\Psi(x) \cong (3/4)^{1/4}/(x - x_0)^{1/2}$ for $x_0 \cong 1$ and $0 < x - 1 \ll 1$ as in the sphere case [see the remark below Eq. (25)].

IV. ADSORPTION AROUND MOVING COLLOIDAL PARTICLES

So far, we have fixed the position of a sphere or a cylinder. We may also suppose colloidal particles in a near-critical fluid [16–20]. Beysens' group [16] observed an increase of the scattered light intensity due to the formation of adsorption layers on colloid surfaces [16], where $\xi_{\rm B}/a \sim 0.1$ typically in their experiments. Such thin layers should remain attached to the particles during their thermal Brownian motions. However, for $a < \xi_{\rm B}$, it is not clear how the adsorption occurs far from the surfaces. Here, we argue that the particle motions should prevent the establishment of long-range absorption profiles.

We consider a colloidal particle with radius a in the strong adsorption condition, $H_1 \gg 1$, where the fluid is at criticality far from it. In this case, we can introduce a space-dependent relaxation time t_ξ of the critical fluctuations around the particle by [35]

$$t_\xi = 6\pi\eta_s\xi(\psi)^3/k_{\rm B}T_c, \tag{44}$$

where $\xi(\psi)$ is the local correlation length in Eq. (4) depending on r as in Eq. (28). The η_s is the viscosity, which may be treated as a constant due to its weak singularity. On the other hand, the particle undergoes Brownian motions, moving a distance of a on the diffusion time,

$$t_a = a^2/D = 6\pi\eta_s a^3/k_{\rm B}T_c, \tag{45}$$

where $D = k_{\rm B}T_c/6\pi\eta_s a$ is the diffusion constant. From Eq. (28), the ratio t_a/t_ξ is larger than 1 for $a < r < 2a$ but is smaller than 1 for $r > 2a$. Hence, by the diffusion, the profile $\psi(r)$ should not be affected in the vicinity ($a < r < 2a$), but it should be largely deformed far from the particle ($2a < r < \xi_{\rm B}$). As a result, for $a < \xi_{\rm B}$, the excess adsorption of a diffusing particle should be significantly smaller than that of a fixed particle in Eq. (31).

As a related experiment, Omari *et al.* [17] determined the hydrodynamic radius $R_{\rm H}$ of colloidal particles with $a = 25$ and 10 nm from their diffusion constant. Remarkably, the effective layer thickness $R_{\rm H} - a$ increased above a on approaching the critical point, where the maximum of $R_{\rm H}$ was about $5a$ for $\xi_{\rm B} \sim 80$ nm. As argued above, the diffuse boundaries of such thick layers should be nonstationary and nonspherical. For not very small colloid densities, the interaction among the particles also appears with increasing the layer thickness. Further experiments are informative to understand these aspects.

We mention simulations on the dynamics of colloidal particles with adsorption layers, which include the hydrodynamic interaction. Furukawa *et al.* [43] found deformations of thick adsorption layers at the critical composition. Yabunaka *et al.* [40] examined the bridging dynamics between two particles at off-critical compositions using the local functional theory, where the adsorption layer remained attached to the surfaces for $\xi_{\rm B} \sim 0.1a$. Barbot and Araki [44] studied aggregation and rheology of a large number of colloidal particles outside the solvent coexistence curve. They observed bridging among the particles at off-critical compositions. However, we need further simulations accounting for the Brownian motions in the case $a < \xi_{\rm B}$.

V. SUMMARY AND REMARKS

We have calculated the order parameter profile $\psi(r)$ around a sphere and a cylinder fixed in a fluid at bulk criticality, where the radius a is longer than the microscopic length a_0. Following de Gennes [6], we have used the local free energy in Eq. (2) and the surface free energy in Eq. (8) with significant surface field h_1.

In Sec. III, setting $\eta = 0$ and $d = 3$, we have solved de Gennes' equation to find the following: (i) The strong adsorption regime is realized when the normalized surface field $H_1(\propto a^{3/2}h_1)$ exceeds 1. (ii) For $H_1 \gg 1$, the surface order parameter $\psi_s = \psi(a)$ grows up to a value $(\propto h_1^{1/3})$ independent of a, which coincides with the one on a planar surface. (iii) We have found the exact profile $\psi \propto (r^2 - x_0^2a^2)^{-1/2}$ $(0 < x_0 < 1)$ around a sphere and the asymptotic decay $\psi \to \psi_{\rm sp} \propto r^{-1/2}$ $(r \gg a)$ around a cylinder. In Appendix A, these expressions become $\psi \propto (r^2 - x_0^2a^2)^{-\beta/\nu}$ around a sphere and $\psi \propto r^{-\beta/\nu}$ around a cylinder, with $\beta/\nu = (d - 2 + \eta)/2$ for general d and nonvanishing η.

In Sec. IV, we have argued that the Brownian motions of colloidal particles strongly affect their thick adsorption layers for $a < \xi_{\rm B}$. The physics in this case has not been examined in the literature. We need to fix a solid sphere or a cylinder in space to confirm the predicted critical long-range adsorption.

We further make critical remarks as follows:

(i) The long-range decay $\psi(r) \propto r^{-(d-2+\eta)}$ around a fixed sphere is of the same form as the correlation function of the order parameter fluctuations at bulk criticality, as has been discussed around Eq. (32). Note that the equation $\Psi'' + (d-1)x^{-1}\Psi' = \Psi^\lambda$ around a sphere $(x = r/a)$ can be solved exactly for $\lambda = (d+2)/(d-2)$ as in Eq. (A4). In particular, at the mean field criticality in three dimensions $(d = \lambda = 3)$, we find $\Psi \cong x^{-1}(2\ln x + A_m)^{-1/2}$ for $x \gg 1$ (A_m being a constant) and $\Psi \propto (x - x_0)^{-1}$ as $x \to x_0$ $(x_0 < 1)$.

(ii) Though we have calculated ψ at the critical composition (for mixture solvents), the preferential adsorption is much enhanced when the solvent component favored by the surface is poorer than the other one in the bulk [30,34,40]. This off-critical enhancement is crucial in the observed phenomenon of colloid aggregation [16,19,20]. In this case, $\psi(r)$ passes through zero at $r - a \sim \xi_{\rm B}$ since $\psi(a) > 0$ and $\psi(\infty) < 0$, leading to bridging phase separation.

(iii) As stressed in Sec. IV, further experiments and simulations are needed to investigate the solvent-mediated colloid interactions in the case $a < \xi_{\rm B}$.

ACKNOWLEDGMENTS

This work was supported by KAKENHI Grant No. 15K05256. A.O. would like to thank D. Beysens for informative correspondence. S.Y. was supported by Grant-in-Aid for Young Scientists (B) (Grant No. 15K17737), Grants-in-Aid for Japan Society for Promotion of Science (JSPS) Fellows (Grant No. 14J03111), and the JSPS Core-to-Core Program "Non-equilibrium dynamics of soft matter and information".

APPENDIX A: PROFILES FOR GENERAL d AND NONVANISHING η AT BULK CRITICALITY

We seek the exact profiles minimizing F in Eq. (2) for general d and nonvanishing η using Eq. (3). In terms of φ in Eq. (11), we obtain the bulk equilibrium relation,

$$(\beta b_0/\nu)^2\nabla^2\varphi = d(d-2)\varphi^{(d+2)/(d-2)}, \tag{A1}$$

and the boundary condition on the surface,

$$\boldsymbol{n}\cdot\nabla\varphi = -(1+\eta_1)^{-1}C_0^{-1}\varphi^{\eta_1}h_1. \tag{A2}$$

Here, we have used Eqs. (3) and (5) with $\eta_1 = \eta/(d-2)$.

First, let the one-dimensional solution of Eq. (A1) be written as $\varphi_{\rm p}(z)$, which behaves as $(z + z_0)^{-1/2}$ with z_0 being a positive constant. From Eq. (11), the order parameter profile $\psi_{\rm p}(z)$ is written as

$$\psi_{\rm p}(z) = \varphi_{\rm p}(z)^{1+\eta_1} = [\beta b_0/2\nu(z+z_0)]^{\beta/\nu}. \tag{A3}$$

Second, for a sphere with radius a, we set $\nabla^2 = d^2/dr^2 + (d-1)r^{-1}d/dr$ in Eq. (A1) to obtain $\varphi_{\rm s}(r) \propto (r^2/a^2 - x_0^2)^{-1/2}$. The profile $\psi_{\rm s}(z)$ is expressed as

$$\psi_{\rm s}(r) = \varphi_{\rm s}(r)^{1+\eta_1} = \left[\beta b_0 x_0 a/\nu\left(r^2 - x_0^2a^2\right)\right]^{\beta/\nu}, \tag{A4}$$

where x_0 is in the range $[0,1]$. Here, in the limits $x_0 \to 1$ and $r/a - 1 \ll 1$, Eq. (A4) leads to Eq. (A3) with replacement $r - x_0a \to z + z_0$ with $z_0 = a(1 - x_0)$.

Third, for a cylinder with radius a, we set $\nabla^2 = d^2/dr^2 + (d-2)r^{-1}d/dr$. In this case, we can find an exact solution $\varphi_{\rm sp}(r)$ only for a special value of h_1 as in Sec. III C (where $d = 3$ and $\eta = 0$). It is expressed as $\varphi_{\rm sp}(r) \propto r^{-(d-2)/2}$ so that

$$\psi_{\rm sp}(r) = \varphi_{\rm sp}(r)^{1+\eta_1} \propto r^{-\beta/\nu}. \tag{A5}$$

Around a cylinder, the profile $\psi(r)$ tends to $\psi_{\rm sp}(r)$ at large $r \gg a$ for any h_1, as shown in Sec. III C.

APPENDIX B: PROFILE AROUND A CYLINDER

We derive the behaviors of $\Psi(x)$ in Fig. 3 in the case of a cylindrical wire. To this end, we rewrite Eq. (33) in terms of $w(x) = (2x)^{1/2}\Psi(x)$ as

$$4x^2w'' = w^5 - w, \tag{B1}$$

where $w'' = d^2w/dx^2$. This is surely satisfied for $w = 1$ as a special solution with $H_1 = 2^{-3/2}$. For any H_1, w tends to 1 at large x. If we linearize Eq. (B1) with respect to the deviation $w_1 = w - 1$, we obtain $x^2w_1'' = w_1$. Thus, for $x \gg 1$, we obtain the algebraic decay,

$$w_1 \cong G_1x^{-\zeta}, \tag{B2}$$

where $\zeta(\zeta+1) = 1$ so $\zeta = (\sqrt{5} - 1)/2$. This then leads to Eq. (38).

W also examine Eq. (B1) in the range $0 < x < 1$ because of Eqs. (36) and (37). In terms of $t = \ln(1/x) > 0$, we rewrite it as

$$\ddot{w} + \dot{w} = -\tfrac{1}{4}(w - w^5) = -\frac{\partial}{\partial w}U(w). \tag{B3}$$

We may regard $w(t)$ as a position of a particle, where $\dot{w} = dw/dt$ is its velocity and $\ddot{w} = d^2w/dt^2$ is its acceleration. Then, $\dot{w}$ in the left-hand side of Eq. (B3) is a friction term. The $U(w)$ is its potential of the form

$$U(w) = w^2/8 - w^6/24. \tag{B4}$$

This potential has a local minimum at $w = 0$, a maximum at $w = 1$, and decays to negative values for $w \gg 1$.

First, if the initial value $w(0)$ at $t = 0$ is smaller than 1, it decreases to 0 obeying $\ddot{w} + \dot{w} \cong -w/4$ for $t \gg 1$. This final decay is overdamped. Thus, for $x \ll 1$, we find

$$w \cong (A_1 + A_2 t)e^{-t/2}, \tag{B5}$$

where A_1 and A_2 are constants. This leads to Eq. (41). Second, if $w(0) > 1$, $w(t)$ grows rapidly obeying $\ddot{w} \cong w^5/4$. Solving this equation yields an explosive solution,

$$w \cong 3^{1/4}/(t_m - t)^{1/2}, \tag{B6}$$

where t_m is a maximum time. This leads to Eq. (40) with $x_0 = e^{-t_m} < 1$. The behaviors (B5) and (B6) excellently agree with the results from numerical calculations.

[1] J. W. Cahn, J. Chem. Phys. **66**, 3667 (1977).

[2] K. Binder, in *Phase Transitions and Critical Phenomena*, edited by C. Domb and J. L. Lebowitz (Academic, London, 1983), Vol. 8, p. 1; H. W. Diehl, *ibid.*, Vol. 10, p. 76; S. Dietrich, *ibid.*, Vol. 12, p. 1.

[3] P. G. de Gennes, Rev. Mod. Phys. **57**, 827 (1985).

[4] M. E. Fisher and P. G. de Gennes, C. R. Acad. Sci. Paris Ser. B **287**, 207 (1978).

[5] M. E. Fisher and H. Au-Yang, Physica A **101**, 255 (1980).

[6] P. G. de Gennes, C. R. Acad. Sci. II **292**, 701 (1981).

[7] M. E. Fisher and H. Nakanishi, J. Chem. Phys. **75**, 5857 (1981).

[8] D. Beaglehole, J. Chem. Phys. **73**, 3366 (1980).

[9] D. Beysens and S. Leibler, J. Phys. (Paris) Lett. **43**, L133 (1982); H. Zhao, A. Penninckx-Sans, L.-T. Lee, D. Beysens, and G. Jannink, Phys. Rev. Lett. **75**, 1977 (1995).

[10] C. Franck and S. E. Schnatterly, Phys. Rev. Lett. **48**, 763 (1982); M. Schlossman, X.-l. Wu, and C. Franck, Phys. Rev. B **31**, 1478 (1985).

[11] G. H. Findenegg and R. Löoring, J. Chem. Phys. **81**, 3270 (1984).

[12] A. J. Liu and M. E. Fisher, Phys. Rev. A **40**, 7202 (1989).

[13] N. S. Desai, S. Peach, and C. Franck, Phys. Rev. E **52**, 4129 (1995).

[14] J. H. Carpenter, J.-H. J. Cho, and B. M. Law, Phys. Rev. E **61**, 532 (2000); B. M. Law, Prog. Surf. Sci. **66**, 159 (2001).

[15] J.-H. J. Cho and B. M. Law, Phys. Rev. Lett. **86**, 2070 (2001).

[16] D. Beysens and D. Esteve, Phys. Rev. Lett. **54**, 2123 (1985); D. Beysens, J.-M. Petit, T. Narayanan, A. Kumar, and M. L. Broide, Ber. Bunsenges. Phys. Chem. **98**, 382 (1994).

[17] R. A. Omari, C. A. Grabowski, and A. Mukhopadhyay, Phys. Rev. Lett. **103**, 225705 (2009).

[18] C. E. Bertrand, P. D. Godfrin, and Y. Liu, J. Chem. Phys. **143**, 084704 (2015).

[19] P. D. Gallagher, M. L. Kurnaz, and J. V. Maher, Phys. Rev. A **46**, 7750 (1992).

[20] H. Guo, T. Narayanan, M. Sztuchi, P. Schall, and G. H. Wegdam, Phys. Rev. Lett. **100**, 188303 (2008); D. Bonn, J. Otwinowski, S. Sacanna, H. Guo, G. H. Wegdam, and P. Schall, *ibid.* **103**, 156101 (2009).

[21] S. Blümel and G. H. Findenegg, Phys. Rev. Lett. **54**, 447 (1985); M. Thommes, G. H. Findenegg, and H. Lewandowski, Ber. Bunsenges. Phys. Chem. **98**, 477 (1994).

[22] O. Di Giovanni, W. Dörfler, M. Mazzotti, and M. Morbidelli, Langmuir **17**, 4316 (2001).

[23] R. Garcia, S. Scheidemantel, K. Knorr, and M. H. W. Chan, Phys. Rev. E **68**, 056111 (2003).

[24] H. W. Diehl and S. Dietrich, Z. Phys. B **42**, 65 (1981); M. Krech and S. Dietrich, Phys. Rev. A **46**, 1886 (1992); G. Flöter and S. Dietrich, Z. Phys. B **97**, 213 (1995).

[25] J. Rudnick and D. Jasnow, Phys. Rev. Lett. **48**, 1059 (1982); **49**, 1595 (1982).

[26] S. Leibler and L. Peliti, J. Phys. C **15**, L403 (1982); E. Brézin and S. Leibler, Phys. Rev. B **27**, 594(R) (1983).

[27] H. W. Diehl and A. Ciach, Phys. Rev. B **44**, 6642 (1991); U. Ritschel and P. Czerner, Phys. Rev. Lett. **77**, 3645 (1996); H. W. Diehl, Int. J. Mod. Phys. B **11**, 3503 (1997); A. Ciach, A. Maciolek, and J. Stecki, J. Chem. Phys. **108**, 5913 (1998).

[28] Z. Borjan and P. J. Upton, Phys. Rev. E **63**, 065102(R) (2001).

[29] S. B. Kiselev, J. F. Ely, and M. Yu. Belyakov, J. Chem. Phys. **112**, 3370 (2000).

[30] R. Okamoto and A. Onuki, J. Chem. Phys. **136**, 114704 (2012).

[31] T. W. Burkhardtt and E. Eisenriegler, J. Phys. A: Math. Gen. **18**, L83 (1985).

[32] R. Holyst and A. Poniewierski, Physica A **149**, 622 (1988); M. P. Gelfand and R. Lipowsky, Phys. Rev. B **36**, 8725 (1987); P. J. Upton, J. O. Indekeu, and J. M. Yeomans, *ibid.* **40**, 666 (1989).

[33] A. Hanke and S. Dietrich, Phys. Rev. E **59**, 5081 (1999).

[34] R. Okamoto and A. Onuki, Phys. Rev. E **88**, 022309 (2013).

[35] A. Onuki, *Phase Transition Dynamics* (Cambridge University Press, Cambridge, 2002).

[36] D. Stauffer, D. Ferer, and M. Wortis, Phys. Rev. Lett. **29**, 345 (1972).

[37] P. C. Hohenberg, A. Aharony, B. I. Halperin, and E. D. Siggia, Phys. Rev. B **13**, 2986 (1976).

[38] After the renormalization of the fluctuations with wave numbers larger than ξ_B^{-1}, the fourth order term in the free energy density becomes $C_0^2 u^* \xi_B^{-\epsilon} \psi^4/4$ in the ϵ method [35], where u^* is a universal number. Some calculations give $A_c = 2^d 6^{-\epsilon/2}/u^* = 18/\pi^2\epsilon$ to first order in ϵ [30].

[39] S. Yabunaka, R. Okamoto, and A. Onuki, Phys. Rev. E **87**, 032405 (2013).

[40] S. Yabunaka, R. Okamoto, and A. Onuki, Soft Matter **11**, 5738 (2015).

[41] P. G. de Gennes, Macromolecules **14**, 1637 (1981).

[42] With respect to the scaling transformation (36), x_0 in Eq. (40) is changed to $x_0' = x_0/\lambda$. Also A_1 and A_2 in Eq. (41) are changed to $A_1' = \lambda^{1/2}(A_1 - A_2 \ln\lambda)$ and $A_2' = \lambda^{1/2} A_2$, while A_3 in Eq. (42) is unchanged.

[43] A. Furukawa, A. Gambassi, S. Dietrich, and H. Tanaka, Phys. Rev. Lett. **111**, 055701 (2013).

[44] A. Barbot and T. Araki, Soft Matter **13**, 5911 (2017).